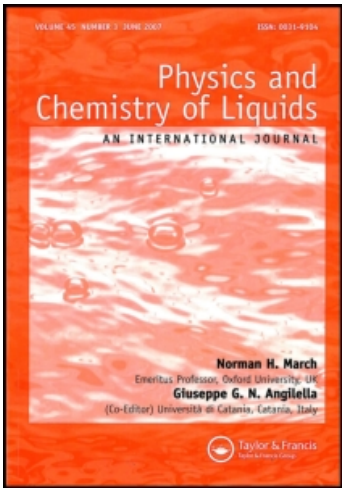

Physics and Chemistry of Liquids
Publication details, including instructions for authors and subscription information:
http://www.informaworld.com/smpp/title~content=t713646857

Mechanical Properties of Liquids: Newtonian and Beyond

D. M. Heyes[a]; N. H. March[b]
[a] Department of Chemistry, University of Surrey, Guildford, Surrey, England [b] Theoretical Chemistry Department, University of Oxford, Oxford, England

To cite this Article Heyes, D. M. and March, N. H.(1994) 'Mechanical Properties of Liquids: Newtonian and Beyond', Physics and Chemistry of Liquids, 28: 1, 1 — 27
To link to this Article: DOI: 10.1080/00319109408029536
URL: http://dx.doi.org/10.1080/00319109408029536

Phys. Chem. Liq., 1994, Vol. 28, pp. 1–27
Reprints available directly from the publisher
Photocopying permitted by license only

REVIEW

Mechanical Properties of Liquids: Newtonian and Beyond

D. M. HEYES* and N. H. MARCH†

* *Department of Chemistry, University of Surrey, Guildford, Surrey GU2 5XH, England*
† *Theoretical Chemistry Department, University of Oxford, 5, South Parks Road, Oxford OX1 3UB, England*

(Received 2 October 1993)

The theory of various mechanical properties of liquids, both Newtonian and non-Newtonian, is reviewed. Especially attention is first paid to viscosity, both shear and bulk, and the relation between them is illustrated by reference to an approximate theory of a hard sphere fluid. Relation of these viscosities to other transport coefficients is then considered, the celebrated Stokes-Einstein relation being one focal point. After a brief summary of molecular dynamical simulation results on Lennard-Jones liquids, a substantial part of the review is devoted to non-Newtonian liquids. In particular, linear viscoelastic response leads to a complex shear modulus, with real part the storage modulus and imaginary part the loss term; simple models for these are summarized. Then substantial attention is given to the results of molecular simulation applied to linear and non-linear transport coefficients of molecular liquids and its extension to the dynamics of colloidal liquids. The article concludes with some proposals for future work in this general area.

KEY WORDS: Viscosities, Stokes-Einstein relation, non-Newtonian liquids.

1 INTRODUCTION

Mechanical properties of liquids include shear and bulk viscosities, compressibility, both isothermal and adiabatic, and related to the latter, the velocity of propagation of sound.

After some brief remarks on the mechanisms of viscous flow in liquids, the topic of viscosity is taken up quantitatively for the model of a dense hard sphere liquid, for which approximate analytical results can be obtained for various transport coefficients. This model, while too primitive for quantitative treatment of any one monatomic liquid, is valuable in (a) estimating bulk viscosity from shear viscosity η, the former still being rather hard to measure in the laboratory, and (b) for forging links with other transport coefficients, eg thermal conductivity λ and also the self-diffusion coefficient D. Any relationship between thermal conductivity and shear viscosity is then investigated for liquid argon. While there is an undoubted correlation, there is substantial temperature dependence of the ratio λ/η, which is predicted to be constant in the hard sphere model.

Therefore, attention is then focussed on a further ('cage') model due to Zwanzig, which is connected with the Stokes-Einstein relation between D and η, but now embraces also the bulk viscosity. The relation of the latter quantity to sound-wave attenuation is emphasized.

The next part of the article is then devoted to the relation between mechanical properties and the dynamical structure factor $S(q, \omega)$ of the liquid. This quantity is, in essence, the probability that a neutron incident on the liquid will transfer momentum $\hbar q$ and energy $\hbar\omega$ to the liquid. The integral over all energy transfers gives the static structure factor $S(q)$, which, when diminished by unity and Fourier transformed, yields the pair distribution function $g(r)$ of the liquid. The long wavelength limit $S(q = 0)$ is related by fluctuation theory to the isothermal compressibility K_T, another basic mechanical property of liquids. Because of the pronounced short-range order in dense liquids like argon near its triple point, $S(0)$ is very much less than unity. It is even smaller for liquid metals, often as low as 0.01 at their melting points.

The hydrodynamic diffusion equation is used, by way of illustration, to set up a formally exact Green-Kubo formula for the coefficient D of self-diffusion, and this is then generalized to give a related formula for a combination of shear and bulk viscosities in terms of the dynamical structure factor.

Because of the need to appeal to hard spheres, and to the 'cage' model, to obtain analytical expressions for transport coefficients, with their obvious quantitative limitations when applied to realistic liquids, a short discussion of time-dependent correlation functions is given in relation to computer experiments on Lennard-Jones liquids. These, of course, afford an alternative to laboratory experiments on dense argon or krypton, but with the advantage that the transport coefficients are calculated from a known, given, pairwise additive force law.

The above discussion is about Newtonian liquids, for which there is a direct proportionality between shear stress and rate of shear. An inevitably more qualitative discussion is added on non-Newtonian liquids, with some experimental facts, plus a few theoretical concepts that seem to point valuable directions for future progress. The article concludes with a brief discussion of the now important technological area of interfacial transport, closely related to interfacial hydrodynamics. The interfacial shear viscosity, defined as interfacial shear stress divided by the rate of shear, can now be measured in the presence of surfactants.

2 MECHANISMS OF TRANSPORT

It is well established that in a liquid the transport of momentum (and energy), as opposed to the transport of matter, occurs by two independent mechanisms, namely the bodily movement of molecules through space and the action of intermolecular forces at a distance. Of these two processes, the former is predominant at low densities while the latter is the important mechanism at the high densities with which we are concerned in this review. The transport properties of monatomic fluids at low densities are well understood through the work[1] of Chapman and Enskog. The dense liquid transport problem is less well understood at the time of writing. This is because in a liquid where the intermolecular potential varies continuously with distance, the collisional momentum (or energy) transport arises from a distortion of the radial distribution function $g(r)$, as emphasized in the early work of Irving and Kirkwood[2]. At the time of writing, no entirely satisfactory approach has been found to allow the calculation of this distortion.

Below, we shall exploit the simplicity of a model liquid of dense hard spheres to calculate the transport of momentum, reflecting the shear viscosity η, and the transport of energy, yielding the thermal conductivity λ. However, before turning to that, we need to say a little about the somewhat less well known bulk viscosity.

2.1 *Compressional (or bulk) viscosity: mechanism and measurement*

Consider first the viscous attenuation of a plane wave in a liquid of shear viscosity η. As the wave travels, there is relative motion of adjacent layers of the liquid and this results in the creation of viscous forces which act against the acoustic pressure of the wave. Energy is taken out of the wave to overcome these viscous forces, a progressive extraction of energy which results in a corresponding progressive decrease in the intensity. When the product of angular frequency ω and relaxation time is very much less than unity, which is usually the case, then the acoustic absorption coefficient, α_1 say, due to shear viscosity, can be shown to take the form (see e.g. Temperley and Trevena[3]):

$$\alpha_1 = \frac{2\omega^2\eta}{3dc^3} \tag{2.1}$$

where d is the mass density of the liquid while c is the velocity of sound.

We can now modify the above formula (2.1) to take account of structural relaxation. This is done by introducing a compressional viscosity, η' say, through rewriting Eq. (2.1) as

$$\alpha_1 = \frac{2\omega^2(\eta + \eta')}{3dc^3}. \tag{2.2}$$

Thus, in principle, one can extract the compressional viscosity η' from measurements of sound-wave attenuation, plus shear viscosity. Of course, in practice, the information that can be extracted depends on error bars on α_1 and η from experiment, and the amount η' contributes in Eq. (2.2) relative to the shear viscosity η.

But it is a fact that the interpretation of such acoustic absorption measurements requires, beyond density and velocity of sound appearing already in Eq. (2.2), accurate knowledge, transcending that equation, of heat capacity and also of other transport coefficients, and in particular thermal conductivity. It may be some time yet, therefore, before one can avoid considerable uncertainties in the final 'experimental' values of compressional viscosity η'.

3 SHEAR AND BULK VISCOSITIES OF DENSE HARD SPHERE LIQUID

We have noted above that, strictly, to calculate the transport of momentum, and hence the shear viscosity η, one must be able to calculate the distortion of the pair function $g(r)$, and that this remains as a largely unsolved problem.

However, as emphasized by Collins and Raffel[4] and by Longuet-Higgins and Pople[5], in a liquid consisting solely of rigid molecules the singular nature of the intermolecular potential permits a finite flux of momentum (or energy) even when the radial distribution function is momentarily isotropic, as it is in equilibrium. It should not, however, be assumed that in a hard-sphere liquid under shear the pair distribution function really is isotropic—in fact the velocity gradient will instantly distort it—but nevertheless by assuming an isotropic distribution function one can make a better than order of magnitude estimate of the transport coefficients, following Longuet-Higgins and Pople[5].

The earliest study of the transport properties of a dense hard-sphere liquid again goes back to Enskog (see the book by Chapman and Cowling[1]). Indeed Enskog developed a modified form of the Boltzmann equation for the single-particle distribution function to apply at high densities. Subsequently Collins and Raffel[4] used the free volume theory of liquids to obtain an expression for the shear viscosity of a hard-sphere liquid which is closely related to the one derived below, following the approach of Longuet-Higgins and Pople[5]. These latter workers demonstrated that it was possible to calculate the collisional contributions to both bulk and shear viscosities in a direct manner by making just two assumptions:

(A) that the spatial pair distribution function depends only on the temperature and density and not on the rate of strain (or temperature gradient) and

(B) that the velocity distribution function of a single particle is Maxwellian with a mean equal to the local hydrodynamic velocity, and a spread determined by the local temperature.

3.1 *Shear viscosity*

Let us consider a situation in which the fluid is subjected to a steady shear represented by

$$\frac{\partial vx}{\partial y} = \frac{-p'}{M} \tag{3.1}$$

all other components of the rate-of-strain tensor being zero. If M denotes the mass of a sphere, p' represents a momentum rather than a velocity gradient. One can now proceed to evaluate the total x-momentum transferred through unit distance in the y-direction in a very short unit of time. This momentum transfer will be due almost exclusively to collisions of pairs of spheres which are already close together at the beginning of the short period of time. Let us denote such a pair of spheres by 1, 2 and let the direction cosines of the unit vector $\mathbf{l}$ along momenta of the line of centres $\mathbf{r}_{12}$ be l_x, l_y and l_z. If the components of the two spheres in the direction $\mathbf{r}_{12}$ are p_1, p_2, then their relative momentum of approach is

$$p = p_1 - p_2 \tag{3.2}$$

Now if $p > 0$, the spheres will soon collide, and when this happens an amount of momentum $p\mathbf{l}$ will be transferred from one to the other. The x component of this

momentum is pl_x and the y-component of the vector $\mathbf{r}_{12}$ is $2al_y$, where a is the radius of a sphere. Moreover the rate of approach of the two spheres is p/M. Therefore the total flux of x-momentum in the y direction arising from collisions is

$$P^c_{xy} = \oint\int_c^\infty h(\omega, p)\frac{2ap^2 l_x l_y}{n} d\omega dp. \tag{3.3}$$

Here $h(\omega, p)\,d\omega$ represents the number of pairs per unit volume within unit small distance of contact having relative momentum p and such that the vector $\mathbf{l}$ lies in the solid angle $d\omega$. The first integration is over all possible orientations while the second is over the positive range of p.

To this point the argument is exact. But to proceed further it is, of course, necessary to insert a form for h. To obtain such a result Longuet-Higgins and Pople[5] assume a form

$$h(\omega, p) = (g_0/4\pi)\phi(\omega, p) \tag{3.4}$$

where g_0 is the equilibrium number of pairs per unit volume within unit (small) distance of contact and $\phi(\omega, p)$ is the probability that spheres 1, 2 have relative momentum p in the direction $\mathbf{r}_{12}$. This form (3.4) has subsumed in it the assumption already referred to that the spatial pair distribution function is independent of the rate of strain. Next, it can be assumed without loss of generality that the fluid velocity is zero at the point of collision of the two spheres. Then the average momentum of the first sphere is $ap' l_y$ in the x-direction and that of the second sphere is $-ap' l_y$. The mean values of p_1, p_2 are therefore $ap' l_x l_y$, $-ap' l_x l_y$ respectively and one can write down their distributions ϕ_1 and ϕ_2 readily since the momentum distribution is assumed to be locally Maxwellian. The distribution of p needed in eqn (3.4) is therefore

$$\phi(\omega, p) = (4\pi M k_B T)^{-1/2} \exp(-(p - 2ap' l_x l_y)^2/4Mk_B T. \tag{3.5}$$

This can be used in Eq. (3.3) to calculate the momentum flux. In evaluating the integral, it is a valid procedure to expand the integrand to only the first power of p', since velocity gradients are assumed small. The result is (Longuet-Higgins and Pople[5]):

$$P^c_{xy} = \frac{8a^2 p'}{15} g_0 \left(\frac{k_B T}{\pi M}\right)^{1/2} \tag{3.6}$$

where g_0 is the value of the radial distribution function $g(r)$ at contact. This can be expressed precisely in terms of the pressure P and the number density N/V to yield for $P^c_{xy}/(p'/M)$ which is simply the shear viscosity η.

$$\eta = \frac{4a}{5}\left(\frac{Mk_B T}{\pi}\right)^{1/2}\left(\frac{P}{k_B T} - \frac{N}{V}\right). \tag{3.7}$$

Before considering this result for the shear viscosity further, let us outline the way the corresponding result for the bulk viscosity can be calculated.

3.2 *Bulk viscosity*

To calculate the viscosity, η_B say, one imagines the fluid to be contracting uniformly at a rate determined by the velocity gradients

$$\frac{\partial v_x}{\partial x} = \frac{\partial v_y}{\partial y} = \frac{\partial v_z}{\partial z} = -p_b'/M \quad \text{say.} \tag{3.8}$$

Considering the fluid velocity to be zero at the point of collision between spheres 1 and 2, the distributions of p_1 and p_2 are now found to be

$$\phi_1(p_1) = (2\pi M k_B T)^{-1/2} \exp(-(p_1 - ap_b')^2/2Mk_B T) \tag{3.9}$$

while $\phi_2(p_2)$ is given by simply replacing the quantity $(p_1 - ap_b')$ in Eq. (3.9) by $(p_2 + ap_b')$. Now the flux of z-momentum in the z-direction is obtained by substituting z for x and y in Eq. (3.5). Using the same form as before for the function $h(\omega, p)$, the corresponding quantity to Eq. (3.6); namely P^c_{zz}, leads to a sum of two terms: one of which is independent of the rate of strain and represents the collisional contribution to the pressure, while the other, which is proportional to the rate of strain, must be interpreted as giving rise to a bulk viscosity. The coefficient of bulk viscosity η_B is, in fact, the pressure decrease divided by the divergence of the rate of strain, which in the present case is just $-3p_b'/M$. The bulk viscosity that results is

$$\eta_B = \frac{4a}{3}\left(\frac{Mk_B T}{\pi}\right)^{1/2}\left(\frac{P}{k_B T} - \frac{N}{V}\right). \tag{3.10}$$

This is seen by comparison with Eq. (3.7) for the shear viscosity of a hard sphere liquid to show that the bulk viscosity η_B is (5/3) of the shear viscosity η.

4 VISCOSITIES CORRELATED WITH OTHER TRANSPORT PROPERTIES

In this section, we shall be concerned with correlations which connect viscosities with other transport coefficients, the most celebrated of these being the so-called Stokes-Einstein relation (see Hansen and McDonald[6]). A useful starting point is again afforded by the hard sphere results for dense liquids, set out in the previous section.

4.1 *Connection between shear viscosity and thermal conductivity*

By quite similar arguments to those set out in section 3 for shear and bulk viscosities, Longuet-Higgins and Pople[5] also calculated the thermal conductivity λ for a dense hard sphere liquid, with the result:

$$\lambda = 2ak_B\left(\frac{k_B T}{\pi M}\right)^{1/2}\left(\frac{P}{k_B T} - \frac{N}{V}\right). \tag{4.1}$$

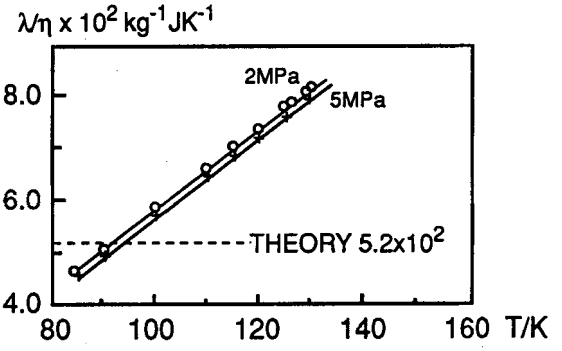

Figure 1 Ratio of thermal conductivity λ to shear viscosity η for liquid argon. Prediction of Eq. (4.2) for hard sphere liquids is also shown. Evidently, variation of λ/η by about a factor of two actually occurs over temperature range plotted.

Combining this with the result (3.7) for the shear viscosity η, one obtains

$$\frac{\lambda}{\eta} = \frac{5k_B}{2M} \tag{4.2}$$

where M is the atomic mass.

As an immediate test of the correlation (4.2), Figure 1 shows a plot of experimental data for argon. There is evidently a substantial variation of the ratio λ/η with temperature at constant pressure, the contant result (4.2) being also shown in the Figure for comparison. We shall return in section 5 to a treatment of transport in a Lennard-Jones fluid like argon, though numerical computation will then be needed. Ascough, Chapman and March[7] have made a somewhat wider study of the prediction that λ/η is constant, and the interested reader is referred to their work.

4.2 Correlation between diffusion and shear viscosity: Stokes law

We referred in section 2 to common elements in the mechanism of transport of momentum and of energy; these are reflected, of course, for hard spheres in the correlation (4.2). While the mechanism is different for mass transport, Louguet-Higgins and Pople[5] have also calculated D for a dense hard sphere liquid as

$$D = \frac{a}{2}\left(\frac{\pi k_B T}{M}\right)^{1/2}\left(\frac{PV}{RT} - 1\right)^{-1}. \tag{4.3}$$

It is then immediately seen from Eqs. (3.7) and (4.3) that

$$D\eta = \frac{2a^2}{5}\frac{Nk_B T}{V}. \tag{4.4}$$

This equation for the product D has the form of the Stokes-Einstein relation: namely $D \sim k_B T/l$, where l is a characteristic length. Evidently $l \sim (V/N)/a^2$ in the hard sphere result (4.4).

4.3 *Generalization of Stokes-Einstein relation to embrace bulk viscosity*

In this section we shall consider the generalization proposed by Zwanzig[8] of the Stokes-Einstein relation to embrace bulk viscosity. It is based, in essence, on a 'cage' model of an atom in a liquid. In such a model, one imagines an atom on which attention is focussed being confined within a limited volume (cage) for an interval of time during which it performs vibrations within the cage. Eventually, by stochastic processes, the cage 'opens up' and the atom 'hops'. Let us follow Zwanzig in subsuming these ideas into an explicit, albeit somewhat oversimplified, model. We shall then see that a generalization of Eq. (4.4) follows.

Let us consider then the motion of the atom performing vibrations about the centre of the cage. The time dependence of a single normal mode contribution varies as $\cos \omega t$, until a cell jump interrupts this motion. Normal modes in different subvolumes are interrupted at different times. Zwanzig[8] accounts for this by introducing a factor of the form $\exp(-t/\tau)$, the waiting time distribution for cell jumps that destroy the coherence of the oscillations in any subvolume V^*. The result is to yield a form for the diffusion constant D given by

$$D = \frac{k_B T}{3MN} \sum_{\omega} \frac{\tau}{1 + \omega^2 \tau^2} \tag{4.5}$$

where the sum is over all the $3N$ normal mode frequencies.

In the absence of much detailed information about the actual frequency distribution (see also below), Zwanzig[8] utilized a Debye spectrum. Treating longitudinal and transverse modes separately, each with its own Debye cut-off q_0:

$$\omega_l(q) = v_l q : \omega_t = v_t q \tag{4.6}$$

for $0 < q < q_0$, v_l and v_t being longitudial and transverse velocities of sound respectively. The cut-off q_0 is chosen such that there are N modes in each branch of the spectrum, so that

$$(4\pi/3)(q_0/2\pi)^3 = (N/V). \tag{4.7}$$

When the sum over frequencies in a single branch of the spectrum is replaced by an integral over q, one arrives, with a minor additional approximation, at the Zwanzig expression

$$D = \frac{k_B T}{3\pi} \left(\frac{3N}{4\pi V} \right)^{1/3} \left(\frac{1}{dv_l^2 \tau} + \frac{2}{dv_t^2 \tau} \right). \tag{4.8}$$

One next notes in Eq. (4.8) that dv_l^2 is an elastic bulk modulus, whereas dv_t^2 is a corresponding shear modulus. As Zwanzig notes, one expects that $dv_l^2 \tau$ and $dv_t^2 \tau$ are actually the longitudinal and shear viscosities η_l and η respectively. Then the self-diffusion coefficient becomes, from Eq. (4.8):

$$D = \left(\frac{k_B T}{3\pi} \right) \left(\frac{3N}{4\pi V} \right)^{1/3} \left(\frac{1}{\eta_l} + \frac{2}{\eta} \right). \tag{4.9}$$

Equation (4.9) can now be rewritten in a form similar to that of the Stokes-Einstein relation (4.4), by defining the volume per atom $\Omega = V/N$. The quantity $\Omega^{1/3}$ is like a 'length per particle' and takes over the role of the characteristic length l below Eq. (4.4). Then one can write, following Zwanzig:

$$\left(\frac{D\eta}{k_B T}\right)\Omega^{1/3} = 0.0658\left(2 + \frac{\eta}{\eta_l}\right) = C', \tag{4.10}$$

where η_l is the longitudinal viscosity, related to $[(4/3)\eta + \eta_B]$. Although the actual value of C', as defined by this equation, clearly depends on the ratio of the shear to the longitudinal viscosity, which as noted above is not known quantitatively in many liquids at the time of writing, Zwanzig notes that C' as defined can only vary between 0.13 and 0.18. Treating C' actually as a constant, Eq. (4.10) has precisely the form obtained by Brown and March[9] discussed in section 5.3 below; at the melting point of metals: see also Andrade[10]. Zwanzig[8] also cites examples of molecular liquids which support the form of Eq. (4.10) but we shall not go into further details here.

Rather, we turn next to establish an intimate link between shear and bulk viscosities on the one hand with neutron scattering on the other. This will be accomplished via the so-called dynamical structure factor $S(q, \omega)$, which we introduce immediately below.

5 DYNAMICAL STRUCTURE FACTOR AND TIME-DEPENDENT CORRELATION FUNCTIONS

Short-range order, so essential in distinguishing the dense liquid state from both the gaseous and solid phases of matter, is described quantitatively by the pair function $g(r)$ of the liquid. This is accessible to measurement via the liquid structure factor $S(q)$ referred to in section 2, which in turn is related to the Fourier transform of $(g(r) - 1)$. Let us now effect a frequency generalization of this static structure factor $S(q)$ such that, for classical liquids to which we confine ourselves throughout this account:

$$S(q) = \int_{-\infty}^{\infty} S(q, \omega)\, d\omega. \tag{5.1}$$

Following van Hove[11], we note that $S(q, \omega)$ is now accessible to inelastic neutron scattering. Essentially, $S(q, \omega)$ is a measure of the probability that a neutron incident on the liquid will transfer momentum $\hbar q$ and energy $\hbar\omega$ to the liquid.

The main object below is to show that, in the hydrodynamic (long-wavelength; long time or low frequency) limit, the dynamical structure factor $S(q, \omega)$ is related quantitatively to a combination of shear and bulk viscosities. To motivate the (initially surprising) form of such a relation, it will prove convenient to return to the self-diffusion coefficient D, connected intimately to viscosity through Eqs. (4.4) or (4.10).

Then, as van Hove especially emphasized, as well as $S(q, \omega)$, in a classical liquid, one can define a quantity $S_S(q, \omega)$ for the motion of a single (s) atom. In turn, this is observable via, now, incoherent neutron scattering as discussed by Egelstaff[12].

The double Fourier transform of this function ($\mathbf{q} \to \mathbf{r}$; $\omega \to t$), namely $G_s(\mathbf{r}, t)$, represents the meanderings of a 'labelled' atom in time. If we have the 'tagged' atom at the origin $\mathbf{r} = 0$ at $t = 0$ then in the hydrodynamic limit referred to above, $G_s(\mathbf{r}, t)$ is characterized by the diffusion equation

$$\nabla^2 G_s(\mathbf{r}, t) = \frac{1}{D}\frac{\partial G_s(\mathbf{r}, t)}{\partial t}. \tag{5.2}$$

With the initial condition specified above, namely $G_s(\mathbf{r}, t = 0) = \delta(\mathbf{r})$, one readily finds the solution of Eq. (5.2) to be

$$G_s(\mathbf{r}, t) = \frac{1}{(4\pi D t)^{3/2}} \exp(-\mathbf{r}^2/4Dt). \tag{5.3}$$

Fourier transforming to get $S_s(q, \omega)$ yields the result

$$S_s(q, \omega) = \frac{Dq^2}{\pi(\omega^2 + (Dq^2)^2)}. \tag{5.4}$$

5.1 *Frequency spectrum (or spectral function) $g(\omega)$*

It is customary to define the frequency spectrum of the liquid by

$$g(\omega) = \omega^2 \lim_{q \to 0} \frac{S_s(q, \omega)}{q^2}. \tag{5.5}$$

While $g(\omega)$ is of considerable interest in its own right, the aim presently is to relate D to $S_s(q, \omega)$ in the hydrodynamic limit. From Eqs. (5.4) and (5.5), it is readily seen that one can obtain the self-diffusion constant D by either of the following procedures:

$$D = \pi \lim_{\omega \to 0} \omega^2 \lim_{q \to 0} \frac{S_s(q, \omega)}{q^2} \tag{5.6}$$

which is a so-called Green-Kubo transport formula, or from

$$g(\omega = 0) = \frac{D}{\pi}. \tag{5.7}$$

The form of $g(\omega)$ in dense liquids is shown schematically in Figure 2.

5.2 *Cusp in frequency spectrum at zero frequency related to shear viscosity*

It will be seen from the above Figure that $g(\omega)$ has a cusp at the origin and the object of the following is to clarify its origin and to relate its quantitative form to the shear viscosity η.

An equivalent form of D to Eq. (5.6), going back essentially to Einstein, is obtained by considering the mean square displacement $\langle r^2 \rangle$ of an atom at long time t. This can be calculated directly from Eq. (5.3) and leads to the result that $\langle r^2 \rangle$ of an atom at long time t tends to $6Dt$. It is instructive to rewrite this result in terms of velocity $\mathbf{v}$ rather than displacement. One has evidently

$$\mathbf{r} = \int_0^t \mathbf{v}(s)\, ds \tag{5.8}$$

and forming the average of r^2 from this Eq. (5.8) one obtains, after some manipulation (see, for example, March[13]):

$$D = \lim_{t\to\infty} \frac{r^2}{6t} = \frac{1}{3}\int_0^\infty \langle \mathbf{v}(0)\cdot\mathbf{v}(t)\rangle\, dt. \tag{5.9}$$

Here we have introduced the so-called velocity autocorrelation function (for more on time-dependent correlations, see section 5.4 below).

From hydrodynamics, and in particular the Navier-Stokes equation (see, for instance, Edwards *et al.*[14]), it can be shown (Ernst *et al.*[15]) that the velocity autocorrelation function falls off at large t with a so-called long-time tail proportional to $t^{-3/2}$. In turn, the Fourier transform of the velocity autocorrelation, related to the frequency spectrum $g(\omega)$ by

$$g(\omega) = \frac{k_B T}{M\pi}\int_0^\infty \frac{\langle \mathbf{v}(0)\cdot\mathbf{v}(t)\rangle}{v(0)^2}\cos\omega t\, dt \tag{5.10}$$

was shown by Gaskell and March[16] to have the small ω expansion:

$$g(\omega) = \frac{D}{\pi} + a_1\omega^{1/2} + 0(\omega) \tag{5.11}$$

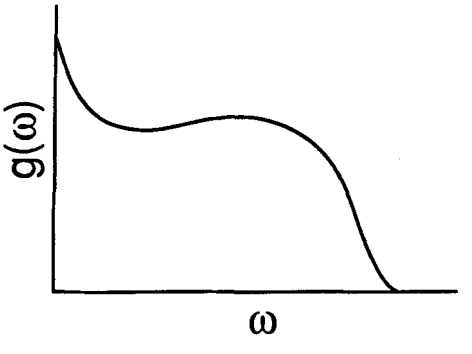

Figure 2 Schematic form of frequency spectrum (or spectral function) $g(\omega)$ as defined in Eq. (5.5). Cusp depicted is made quantitative in Eqs. (5.11) and (5.12). The value of $g(\omega)$ at $\omega = 0$ is D/π, with D the coefficient of self-diffusion.

where

$$a_1 = -(2\pi)^{1/2}\frac{2}{3\rho}\left[4\pi\left(D+\frac{\eta}{\rho M}\right)\right]^{-3/2}\frac{k_B T}{M\pi}, \tag{5.12}$$

with M the atomic mass. This result for a_1, the coefficient of the term $\omega^{1/2}$ in the expansion (5.11), makes quantitative the form of the cusp depicted in Figure 2. It is clear that though $g(\omega)$ was introduced through the study of the meanderings of a single atom, the cusp contains not only the expected dependence on the coefficient of self-diffusion D but also carries knowledge of the shear viscosity η.

5.3 *Green-Kubo formula for viscosities: application to liquid metals at melting*

There is an analogous formula to Eq. (5.6) involving $S(q,\omega)$ rather than just the self-contribution $S_s(q,\omega)$. This takes the form (see, for example Egelstaff[12]):

$$\frac{4}{3}\eta + \eta_B = \frac{\pi M^2}{k_B T}\lim_{\omega\to 0}\omega^4 \lim_{q\to 0}\frac{S(q,\omega)}{q^4}. \tag{5.13}$$

By arguments involving the assumption of a Debye frequency, Brown and March[9] obtained an approximate formula for liquid metals at the melting point. Specializing to the shear viscosity, this takes the form

$$\frac{\eta}{T_m^{1/2} M^{1/2} \rho^{2/3}} = \text{constant} \tag{5.14}$$

where T_m is the melting temperature and ρ is the atomic number density N/V. Choosing the constant in accord with the early work of Andrade[10] there is excellent agreement between Eq. (5.14) and experiment, as shown in Table 1. There is close connection here with the work of Zwanzig embodied in Eq. (4.10) when D is obtained with similar approximations (Brown and March[9]; March[17]).

5.4 *Computer simulation of viscosities in Lennard-Jones fluids*

While the Green-Kubo formulae for D, and for the combination of viscosities in Eq. (5.13) are formally exact, applications using analytical methods, to date, are all

Table 1 Shear viscosities of liquid metals near melting temperature (in 10^{-2} poise)

	Li	*Na*	*K*	*Rb*	*Cs*	*Cu*	*Ag*	*Au*	*In*	*Sn*
experiment	0.60	0.69	0.54	0.67	0.69	4.1	3.9	5.4	1.9	2.1
theory (Eq. (5.14)	0.56	0.62	0.50	0.62	0.66	4.2	4.1	5.8	2.0	2.1

After Brown and March[9]

invoking subsequent approximations; eg to reach a result like Eq. (5.14). In deriving this result, a fairly well defined Debye frequency has been assumed at the higher 'edge' (see Fig. 2) of the frequency spectrum $g(\omega)$. This assumption is best for simple liquid metals with relatively soft cores and with long-range pair potentials. It is less well suited to treat argon, and similar Lennard-Jones liquids. Therefore, in this section we shall refer to computer experiments on such liquids, which are conveniently carried out via time-dependent correlation functions, as set out below. Molecular dynamics computer simulation, *MD*, was first applied to Lennard-Jones fluids in a seminal paper by Rahman[18]. Until then all the *MD* simulations had been carried out using idealized molecular fluids with discontinuous potentials (hard spheres and square wells for example). Levesque *et al.*[19] first used the technique to calculate the transport coefficients of these liquids. The shear viscosity (see the next section), the bulk viscosity and the thermal conductivity were evaluated using Green-Kubo formulae (compare Eqs. (5.6) and (5.13)). For example, if p denotes $(1/3)(p_{xx} + p_{yy} + p_{zz})$, then the formula for bulk viscosity η_B is

$$\eta_B = \frac{V}{9k_B T}\int_0^\infty dt(\langle p(t) - \langle p\rangle)(p(0) - \langle p\rangle)\rangle. \tag{5.15}$$

Similarly, the thermal conductivity λ is, in terms of heat flux **J**:

$$\lambda = \frac{V}{3k_B T^2}\int_0^\infty dt\langle \mathbf{J}(t)\cdot\mathbf{J}(0)\rangle. \tag{5.16}$$

Since then the technique has been applied numerous times to cover essentially the whole of the Lennard-Jones fluid phase diagram. Levesque and Verlet[20] recently returned to their original study with more extensive simulations and concluded that the (generally accepted[21]) too large value for the shear viscosity at the state $\rho = 0.8442$ and $T = 0.722$ of 4.0 ± 0.1 (LJ reduced units) was due to a long-lived metastable state in the original calculations. The simulations of Borgelt *et al.*[22] and Heyes[23] are perhaps the most extensive LJ simulations of the transport coefficients collected in one place. The data for all the tranport coefficients fits reasonably well to a range of analytical approaches, including a variously closed memory function expansion of the time-correlation function[24,25]. The success with respect to kinetic theories such as Enskog is quite acceptable[23]. However, the mean field kinetic theory based on a conceptual separation of the dynamics into 'hard' and 'soft' collisions is not very good in general[22]

6 NON-NEWTONIAN FLUIDS

So far in this article, we have been concerned solely with liquids that obey Newton's law of constant viscosity. For such a *Newtonian* liquid, the shear viscosity, η, is a constant at given (T, P) and is independent of shear rate. The shear stress, σ_{xy}, varies with shear rate, $dv_x/dy = \dot{\gamma}$ as,

$$\sigma_{xy} = \eta\dot{\gamma}. \tag{6.1}$$

The shear stress is proportional to the shear rate (we assume laminar or turbulent-free flow). Examples of Newtonian liquids are many pure single-phase liquids of low molecular weight, e.g., water. In such liquids, viscous dissipation can be regarded as being due to collisions between fairly small molecules. The shear rate imposes such a small perturbation on the liquid that it can be described in terms of a first order perturbation about the equilibrium state. In fact more properly,

$$\begin{aligned}\sigma_{xy}(\dot{\gamma}) &= \sigma_{xy}(0) + \dot{\gamma}\frac{\partial \sigma_{xy}(0)}{\partial \dot{\gamma}} + O(\dot{\gamma}^2) \\ &= \sigma_{xy}(0) + \eta\dot{\gamma} + O(\dot{\gamma}^2).\end{aligned} \tag{6.2}$$

As the time average of the off-diagonal of the stress tensor at zero shear rate is zero *i.e.*, $\langle \sigma_{xy}(0) \rangle = 0$ then Eq. (6.2) reduces to Eq. (6.1). The general expansion of Eq. (6.2) does however provide the framework for non-linear response. It is useful to attach a timescale, $\tau_s = \dot{\gamma}^{-1}$ to a shear rate, which can be considered to be a 'disruption' time-scale. The time scale for stress relaxation in the liquid state, τ_r can be viewed as the time it takes a typical molecule to diffuse a distance of order its mean diameter, σ. If $\tau_r/\tau_s \ll 1$ the liquid is in the small perturbation ('Newtonian') limit. However, if $\tau_r/\tau_s \gg 1$ then the liquid molecules are not able to remain close to be equilibrium state at this shear flow rate, and there are deviations from Eq. (6.1) and higher order terms in Eq. (6.2) have to be considered. This is called *non-Newtonian* flow and its study is termed *rheology*. In fact, the whole stress tensor, σ has to be considered as the off-diagonal shear stresses couple to the diagonal elements. The diagonal elements of the stress tensor, $\sigma_{\alpha\alpha}$, change under shear. Non-Newtonian fluids typically require large slowly diffusing molecules, such as polymer melts and colloidal liquids containing of solid particles in excess of 0.1μm in diameter. There is a surprisingly large number of non-Newtonian fluid in every-day life (e.g., tomato ketchup and domestic abrasive cleaning fluids are two examples). Water is Newtonian because $\tau_r \sim 10^{-12}$ s, and as it is rare to encounter shear rates in excess of $10^6\,s^{-1}$ then $\tau_r/\tau_s \ll 1$. However for the macro-molecular liquids τ_r can increase so that $\tau_r/\tau_s \gg 1$ is readily achieved.

The history of the sample is often an important parameter in determining non-Newtonian behaviour, especially, for polymeric liquids (although often a steady state can be achieved in which case the history of the sample can be neglected in practice). In general, the stress tensor depends on a range of parameters $\underline{\sigma}(t, P, T, \gamma, \dot{\gamma}, \ldots)$, where $\gamma = \int_0^t dx\,\dot{\gamma}(x)$ is the shear strain. An analytic relationship between the stress tensor, $\underline{\sigma}$ and these parameters is called the *constitutive* equation. Rheology as widely practised still relies on empirical constitutive equations of the general form,

$$\sigma_{xy} = \sigma_y + \dot{\gamma}^n \eta_p, \tag{6.3}$$

where σ_y is the so-called *yield* stress, which is the minimum stress that must be applied to the liquid before it will flow. The exponent, n allows for a range of non-Newtonian responses: $n = 1$, pseudo-Newtonian with an apparent viscosity, η_p called the plastic viscosity (Eq. 6.3) with $\eta = 1$ is widely known as the Bingham fluid). For $n < 1$ the

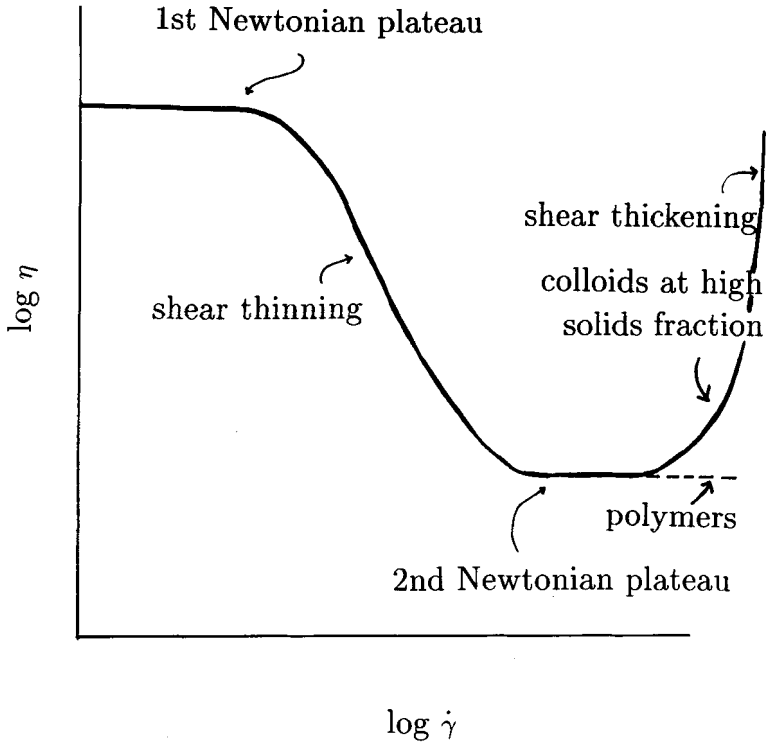

Figure 3 A schematic diagram showing a typical rheological flow curve for a liquid.

apparent viscosity $\sigma_{xy}/\dot{\gamma}$ decreases with increasing shear rate- the liquid is said to be *shear thinning*. If $n > 1$ the liquid is said to be *shear thickening* or 'dilatant', usually a problem encountered with colloidal liquids at high shear rates. At high shear rates the viscosity is often seen to level off to a plateau value. This is observed for polymer solutions, melts and colloidal suspensions. The latter at high solids fractions *ca.* 50%, show the additional dilatant behaviour (see Fig. 3). Shear thinning and shear thickening are associated with some form of internal reordering of the molecules in the bulk of the liquid, in a manner that facilitates flow under the applied shear stress or strain rate. The viscosity of all non-Newtonian liquids will approach a limiting value (if one waits long enough to take the measurement), which is called the Newtonian viscosity, η_0. The viscosity is then given by Eq. (6.1).

Often time or equivalently, 'history' is an essential parameter to include in the description of the liquid. This can arise in two ways. The liquid can be essentially fluid-like in behaviour, and the apparent viscosity, calculated from Eq. (6.3) for example, would be a function of time (the shear thinning form of this is known as *thixotropy*). However, even in the Newtonian strain rate region, where there is a minor perturbation of the liquids internal structure, time can still be an important parameter in characterising the liquid. The application of an oscillatory shear strain to a liquid can excite a *viscoelastic* response, which means that the liquid behaves partly as a classical fluid with no 'memory' of its past history, and partly as an elastic medium in which the

liquid can 'store' elastic energy of deformation which can be recovered on release of the sample by the deforming element. The strain on the sample, $\gamma(t)$ is given by,

$$\gamma(t) = \gamma_0 \cos \omega t \tag{6.4}$$

where γ_0 is the strain-amplitude. Providing the strain amplitude is sufficiently low, typically $\gamma_0 < 0.03$, the structure of the liquid is not significantly disrupted. This linear viscoelastic response is usually represented as a complex shear modulus.

$$G^*(\omega) = G'(\omega) + iG''(\omega), \tag{6.5}$$

where $G'(\omega)$ is the storage modulus and $G''(\omega)$ is the loss modulus, which measure the solid-like and fluid-like characteristics of the liquid respectively at a particular exciting frequency, ω. Consider a step of unit strain applied to the liquid at time $t = 0$. The shear stress in the sample will build up instantaneously and then decay to zero with time. This defines a stress relaxation function, $C_s(t)$. The Maxwell model for a classical viscoelastic fluid defines a $C_s(t)$ as a single exponential with a decay time, $\tau = \eta_0/G_\infty$,

$$C_s(t) = G_\infty \exp(-t/\tau). \tag{6.6}$$

G_∞ is the elastic modulus of the solid aspect of the liquid. In terms of the shear stress relaxation function we have,

$$G^*(\omega) = i\frac{V}{k_B T}\int_0^\infty C_s(t)\exp(-i\omega t)\omega dt. \tag{6.7}$$

which gives,

$$G'(\omega) = \frac{G_\infty(\omega\tau)^2}{1+(\omega\tau)^2}, \tag{6.8}$$

and

$$G''(\omega) = \frac{G_\infty(\omega\tau)}{1+(\omega\tau)^2}. \tag{6.9}$$

So far the discussion of non-Newtonian flow has been phenomenological. In recent years, molecular simulation has been useful in improving our understanding of non-Newtonian liquids from the results of the simulations themselves and from the stimulus the technique has given to advancing the statistical mechanics of the non-equilibrium state.

6.1 Molecular Simulation

The first appearance of rheology (interpreted in its broadest sense) in molecular simulation was in the 1960s, when a *non-intrusive* method was used to compute the

Newtonian viscosity, η_0, of molecular fluids using molecular dynamics (MD). The newtonian viscosity was calculated from the *equilibrium* trajectories of the molecules—simply by monitoring the time decay of shear stress fluctuations in an *unsheared* sample. The Newtonian shear viscosity, η_0, is given by a Green-Kubo formula (compare Eq. (5.9) for D):

$$\eta_s = (V/k_B T) \int_0^\infty \langle \sigma_{\alpha\beta}(0)\sigma_{\alpha\beta}(t)\rangle \, dt, \tag{6.10}$$

where V is the volume containing N molecules, T is the temperature. For monatomic fluids the microscopic definition of the stress is,

$$\sigma_{\alpha\beta} = -\frac{1}{V}\left(\sum_{i=1}^{N} p_{\alpha i} p_{\beta i}/m_i - \sum_{i=1}^{N-1} \sum_{j>i}^{N} (r_{\alpha ij} r_{\beta ij}/r_{ij}) \frac{d\phi(r_{ij})}{dr} \right), \tag{6.11}$$

where p is the α component of the momentum of an arbitrary particle i of mass m_i and $r_{\alpha ij}$ is the α component of $\underline{r}_{ij}$, the vector separating the centres of the two molecules i and j, and $\phi(r)$ is the interaction potential between the molecules. In the simulation the function in the $\langle \cdots \rangle$, called a time correlation function, is calculated. The integral in Eq. (6.10) is performed at the end of the simulation.

Experimentally, viscosity is measured by applying a strain rate and measuring the stress in the fluid. It is only under these circumstances that departures from purely newtonian behaviour can be achieved. In the early 1970s a range of so-called Non-equilibrium Molecular Dynamics, (NEMD), techniques were developed to apply a finite strain rate to molecules in the molecular dynamics cell. Gosling *et al.*[26] published the first paper to observe by *MD* shear thinning of a molecular fluid under shear, by applying an oscillatory shear rate field across the simulation cell. There was an integer number of wavelengths of the shear velocity profile in the gradient direction to allow full periodic boundary conditions with no velocity discontinuity at the boundary (node point). Another influential publication[27] introduced shear flow in the MD cell by sandwiching it between two fluid walls translating in opposite directions. Although this bears a close resemblance to the experimental situation, it is fair to say that this boundary-driven flow method has not found wide use by the molecular simulation community because it is difficult to disentangle the ordering effects of the boundary from the inherent rheology of the fluid, which is present in bulk laminar flow. The simulation cells are too small to obtain a reasonably large bulk region in the centre of the cell far away from the walls. Boundary-free or homogeneous shear schemes have not found more favour, although with improvements in computer power they could become popular again in the future (especially with the continual interest in 'wall-slip' and other boundary effects).

Pseudo-bulk flow can be achieved in molecular simulation using an ingenious modification of the periodic boundary condition convention[28]. These 'sliding image' periodic boundary conditions are implemented by defining the shear flow (x) linear momentum of a molecule in the k-th cell image of a box particle in the shear-gradient (y) direction by,

$$p_x^k = p_x^0 + k\dot{\gamma} L \tag{6.12}$$

where L is the cell side-length and $k = 0, \pm 1, \pm 2 \ldots$. Shear flow can be superimposed on the molecular liquid using the so-called SLLOD equations of motion[29]:

$$\dot{\underline{r}} = \underline{p}/m + \dot{\gamma}\underline{\hat{x}} \tag{6.13}$$

$$\dot{\underline{p}} = m\ddot{\underline{r}} - \dot{\gamma}p_y\underline{\hat{x}} - \alpha\underline{p}, \tag{6.14}$$

where $\underline{\hat{x}}$ is the unit vector in the x-direction. Equation (6.13) represents the extra displacement in the flow (x) direction caused by the shear flow. Equation (6.14) is the Newton equation of motion modified to include the inertial effect of the imposed shear flow. The apparent shear viscosity is calculated using Eq. (6.1). The last term builds in a thermostat to the equations of motion, which is essential to take out the dissipated heat generated by the shear flow. In order to obtain statistically significant shear stresses the applied shear rate has to be $\sim 10^{12}\,s^{-1}$, which is enormous by normal laboratory standards. A range of different prescriptions for $\alpha(t)$ was developed in the 1980s, e.g., gaussian thermostat[30], PUT thermostat[31] and Nosè-Hoover thermostat[32].

At very high shear rates the molecular liquids were observed to reorganise into a quasi-lattice like structure composed of tubes of particles (*'strings'*) flowing along the streaming (flow) direction. A projection of these tubes in the gradient-vorticity plane (yz) revealed a distorted hexagonal lattice. The strings were observed in $2D$ to disappear on replacing the gaussian by the so-called profile unbiased thermostat (PUT)[31]. Since then the use of *NEMD* as a probe of non-equilibrium phase diagrams has been controversial because of the influence of the thermostatting procedure on the structures formed at very high shear rates (well into the second Newtonian plateau). NEMD is a useful route to the Newtonian viscosity, however, by taking the $\eta(\dot{\gamma})$, $\dot{\gamma} \to 0$ limit. NEMD has also been used to calculate the distortion in the radial distribution function, and the change in thermodynamic properties of the equilibrium fluids, in the near-Newtonian region before excessive shear thinning leads to these long range structures. In this mildly shear thinning regime all the thermostats give statistically indistinguishable results.

Under shear flow the pair radial distribution departs from spherical symmetry (compare section 3). The function, $g(\mathbf{r}, \dot{\gamma})$ has the form[33]

$$g(\mathbf{r}, \dot{\gamma}) = g(r, 0) - \varepsilon(xy/r^2)(dg(r, 0)/dr) + O(\varepsilon^2) \tag{6.15}$$

where $\varepsilon = \tau\dot{\gamma}$ and τ is a characteristic relaxation time for the equilibrium stress. ε is a recoverable strain which has to be obtained from the simulation (this is where the many body dynamics enters the formulation). To first order, the distortion of $g(r)(= g(r, 0))$ only affects the shear (xy) plane. The shear stress and hence viscosity could be calculated[33] from Eq. (6.15) but it is easier to use the direct route of Eq. (6.1). For simple (e.g., Lennard-Jones) liquids the shear viscosity and thermodynamic quantities have been observed to have a simple asymptotic behaviour[34] with shear rate as $\dot{\gamma} \to 0$ (provided the state is not too close to the triple point[35]). In three dimensions,

$$\eta(\dot{\gamma}) = \eta(0) - A(\dot{\gamma})^{1/2}, \tag{6.16}$$

$$P(\dot{\gamma}) = P(0) + A(\dot{\gamma})^{3/2}, \tag{6.17}$$

$$E(\dot{\gamma}) = E(0) + A(\dot{\gamma})^{3/2}. \tag{6.18}$$

Similarly, for oscillatory shear in the linear response region,

$$\hat{\eta}(\dot{\gamma}) = \eta(0) - A(i\omega)^{1/2}, \tag{6.19}$$

and

$$\eta(\mathbf{q}) = \eta(0) - A(\mathbf{q})^{3/2}, \tag{6.20}$$

for wave vector $\mathbf{q}$ and where $A(\rho, T)$ is a different state point dependent constant in each case. There do appear to be departures from this generic behaviour close to the triple point itself[35].

A major advance by Evans and Morriss was to extend the Green-Kubo formula to non-equilibrium shear flow[36]. Consider a liquid that is sheared from a time $t = 0$. The shear stress develops along a non-equilibrium trajectory, $\sigma^*_{xy}(t)$ (where the * denotes a non-equilibrium state). They defined a transient time correlation function, $\langle \sigma_{\alpha\beta}(0)\sigma^*_{\alpha\beta}(t)\rangle$, which can be used to evaluate the non-newtonian viscosity as a function of shear rate,

$$\eta(t, \dot{\gamma}) = (V/k_B T)\int_0^t \langle \sigma_{\alpha\beta}(0)\sigma^*_{\alpha\beta}(t)\rangle \, dt, \tag{6.21}$$

This relates the time-dependent apparent viscosity to a correlation between fluctuations in stress in the equilibrium and non-equilibrium states. (In the limit $t \to \infty$ we have $\eta(\dot{\gamma})$.) Equation (6.21) is valid for *arbitrarily* large shear rates and can be generalized to specify normal pressure differences.

A recent application of homogeneous shear NEMD investigated the shear thinning of n-butane[37]. The main problem with NEMD currently is that computer power limits it to fairly small molecules by rheogical standards, which only start to noticeably shear thin at $\dot{\gamma} \sim 10^{12}\,s^{-1}$. At these shear rates even during a typical simulation of tens of picoseconds there is appreciable shear heating, which has to be thermostatted out in some *ad hoc* manner. The consequences of this have still not been fully resolved. We have to wait for increases in computer power of several orders of magnitude before we can realistically plan to simulate at experimentally realized shear rates ($< 10^6\,s^{-1}$), and still get statistically reasonable properties, before *NEMD* becomes a widely used tool.

6.2 *Colloidal Liquids*

While *NEMD* was being developed to investigate molecular fluids, a parallel activity in the modelling of another class of non-Newtonian molecules was being devised and improved. In the mid-1980s Brownian Dynamics, BD, simulation was developed to calculate the rheology of model colloidal dispersions/suspensions. The technique is structually similar to NEMD except that the equations of motion are Langevin rather than Newtonian, which causes the particle motion to be heavily damped. The particle trajectories in the simulation are presumed to be thermostatted by the solvent. Therefore there is no concept of a 'thermostat' in *BD*.

The dynamics of colloidal systems can be interpreted in the light of essentially two characteristic time-scales. The velocity of the colloidal particle fluctuates on a 'Brownian time scale', $\tau_B = m/\xi$, where m is the Brownian particle's mass and ξ is the Stokes friction coefficient (for stick boundary conditions, $\xi = 3\pi\eta_s\sigma$, where η_s, is the solvent viscosity and σ is the diameter, this time, of the Brownian particle). The timescale, τ_B, is many orders of magnitude smaller than the time it takes the particle to move a distance of order its diameter, $\tau_r \sim \sigma^2/D_0$. D_0 is the self-diffusion coefficient of the colloidal particle at infinite dilution ($D_0 = k_B T/\xi$). At very short times a colloidal particle diffuses in an approximately static configuration of surrounding molecules. This is called the 'short time' regime. In the time, t range, $\tau_r \gg t \gg \tau_B$ the self-diffusion coefficient is essentially constant and is called the short time diffusion coefficient, D^S. At longer times, after a particle has diffused a distance of order its diameter, the diffusion process has been slowed down by the interaction of the particle with its cage of particles. The hindered passage of the particle through its cage of surrounding particles slows down its rate of progress, resulting in the diffusion coefficient in this 'long-time' regime falling below the value of D^S. As $t \gg \tau_r$ the diffusion coefficient tends to a constant value, which is called the 'long-time' self-diffusion coefficient D^L. The short time diffusion coefficient has been measured by multiple light scattering[38] while the long time diffusion coefficient is amenable to a wider range of techniques including fluorescence recovery[39] and photon correlation spectroscopy[40,41].

Both D^S and D^L depend on solids volume fraction. The difference between D^S and D^L is some measure of to what extent a colloidal particle is retarded by coupled solvent-mediated forces and particle migration at long times. In the limit of the volume fraction $\phi \to 0$,

$$D^L = D_0(1 - a\phi) \quad t \gg \tau_r, \tag{6.22}$$

and $\phi = \pi N\sigma^3/6V$. There is a range of values for the constant a in the literature; analytic values of a depend on the level of the dynamical approximation, ranging between $-0.08 < a < -2.625$ for example[42]. There have been experimental measurements of the volume fraction dependence of D^S and D^L over the whole liquid range[38,40]. $D^L/D_0 < 0.1$ at the volume fraction at which crystallization takes place[43].

Both atomic and colloidal fluids can be represented by an equivalent hard-sphere fluid, on assignment of an effective hard-sphere diameter, σ to the real particle[44,45]. The density dependence of the self-diffusion coefficient of the hard-sphere fluid is now well-known, with several analytic fits in the literature. For N hard-spheres in volume V, we define a reduced number density, $\rho = N\sigma^3/V$. A fit to simulation data given by Speedy[46] is,

$$D = D_{00}\left(1 - \left(\frac{\rho}{1.09}\right)\right)(1 + \rho^2(0.4 - 0.83\rho^2)). \tag{6.23}$$

Erpenbeck and Wood[47] have fitted their MD hard-sphere simulation data to the expression

$$D = D_E(1 + a_1\rho + a_2\rho^2 + a_3\rho^3), \tag{6.24}$$

where $a_1 = 0.038208154$, $a_2 = 3.182808$ and $a_3 = -3.868771766$. Both Eqs. (6.23) and (6.24) include a reference self-diffusion coefficient. The diffusion coefficient for an ideal hard sphere gas, D_{00}, is determined from kinetic theory to be,

$$D_{00} = 3(k_B T/\pi m)^{1/2}/8\rho\sigma^2, \tag{6.25}$$

and D_E is the Enskog-theory extension of these basic asumptions to finite density,

$$D_E = 1.01896 D_{00}/g(\sigma), \tag{6.26}$$

where $g(\sigma)$ is the value of the pair radial distribution function at the contact of the spheres (compare section 3.1).

In the context of colloidal liquids Eqs. (6.23) and (6.24) are conceptually unsatisfactory, because they use a reference self-diffusion coefficient which is based on the kinetic theory of gases in the limit of zero density, D_{00} or alternatively, its finite density extension, D_E. There is no reason to expect the ideal gas to be pertinent to the colloidal state. Nevertheless, the behaviour of the 'molecular' hard-sphere fluid at finite densities should, in some sense, still be relevant to colloids because, as volume fraction increases, excluded volume effects should act in both the molecular (*i.e.*, hard-sphere) and colloidal liquids to slow down self-diffusion.

An alternative representation of hard-sphere molecular dynamics data, developed from the pioneering work of Hildebrand[48], by Dymond[49], and the others, *e.g.*, ref[50], has similarities with the behaviour of colloidal liquid. Significantly, it does not use the kinetic theory of gases as its basis,

$$D/D_{00} = 1.271\rho(\rho_0/\rho - 1.384)/\rho_0, \tag{6.27}$$

where $\rho_0 = 2^{1/2}$ is the close-packed density of the f.c.c. crystal. This formula is an empirical fit to simulation data which emphasises the dominance of excluded volume effects at high density. The coefficient, D_{00} does appear in Eq. (6.27) to confer a realistic temperature dependence to D but otherwise makes no attempt to go over to the low density limit correctly. The formula in Eq. (6.27) has a low density limit that is not that of the ideal gas. Equation (6.27) is alternatively expressed in terms of the volume fraction,

$$D/D_{00} = 1.271 - 2.37557\phi. \tag{6.28}$$

Equation (6.28) has the limit $D \to 0$ at volume fraction of 0.54, which is equal to the solid density at melting for a hard-sphere system.

Because of the approximate treatment of the solvent, the basic equations of motion for N-interacting Brownian particles are not Newton's equations but ($3N$ coupled) Langevin equations, with an *assumed* extension ot include interacting particles[51].

$$\dot{\mathbf{p}} = -\xi\mathbf{p} + \mathbf{R} + \mathbf{F}, \tag{6.29}$$

where $\mathbf{p}$ is the momentum of the Brownian particle, $\mathbf{R}$ is the Brownian force on the colloidal particle, which is represented by a normally distributed random number. $\mathbf{F}$ is

the systematic or direct force between the colloidal particles (including any external force). The time average of a dynamical quantity obtained from a phase space trajectory generated by the Langevin equations is equivalent to the phase space distribution average obtained from the Fokker-Planck equation. The stationary solution of the Fokker-Planck equation is the canonical distribution function. By virtue of this fact, static properties of the Brownian particle system are not influenced by hydrodynamic interactions and are the same as calculated from canonical *MD* or *MC* simulations for a system of particles with the same interparticle interactions. It should be stressed, however, that presence of a solvent will modify quite dramatically the dynamics of the particles. Consequently the dynamical properties of a Brownian particle system and its MD counterpart are quite different (The reason for that is that the time evolution in these two systems is determined by the different dynamic operators[52]). For most treatments of the dynamics of interacting Brownian particles, only the configurational evolution, which proceeds on a timescale much greater than τ_B, is relevant. In this case the Langevin equations reduce to the "position Langevin equation". The associated equation of motion for the configurational distribution function is the Smoluchowski equation. The Langevin/Smoluchowski position level of equations, like the momentum Langevin/Fokker-Planck level equations, produces canonical averages which, in the case of static quantities, are independent of hydrodynamic interactions and are equal to the *MD* or *MC* averages. This independence of the nature of the simulation method (*MD*, *MC* and *BD*) for static properties provides a good consistency test of the simulations.

Brownian dynamics simulations are based on the position Langevin equation. If many-body hydrodynamic interactions are neglected this equation leads to the following position updating algorithm for the particle positions in time-steps, h,[53]

$$\mathbf{r}_i(t+h) = \mathbf{r}_i(t) + \frac{D_0}{k_B T}\mathbf{F}_i(t)h + \Delta\mathbf{r}_i(t,h) \tag{6.30}$$

where $i = 1, \ldots, N$ are the particle labels, $\mathbf{F}$ is the systematic or direct force between the colloidal particles (including any external force) and $\Delta\mathbf{r}$ is the random displacement sampled from a gaussian distribution of zero mean and variance $\langle \Delta r^2 \rangle = 6D_0 h$. For colloidal particles of diameter in excess of 0.1 μm, $\tau_B \ll \tau_r$, so we can choose a timestep h such that $\tau_B \ll h \ll \tau_r$. Then it can be shown[33] that the Langevin equation is equivalent to the following colloidal particle position update algorithm:

$$r_x(t+h) = r_x(t) + (F_x(t) + R_x(t,h))h/m\xi + \dot{\gamma}(t)hR_y, \tag{6.31}$$

$$r_y(t+h) = r_y(t) + (F_y(t) + R_y(t,h))h/m\xi, \tag{6.32}$$

$$r_z(t+h) = r_z(t) + (F_z(t) + R_z(t,h))h/m\xi. \tag{6.33}$$

The shearing of the liquid is implemented via the $\dot{\gamma}(t)$ term in Eq. (6.31). The random displacement $\delta_x = R_x h/m\xi$ is related to the infinite-dilution self-diffusion coefficient, D_0, by

$$\langle \delta_x^2 \rangle = 2hD_0. \tag{6.34}$$

Just as for *NEMD* configurational averages are computed from values determined at each time step. A number of models which attempt to include many-body hydrodynamics have appeared recently employing a diversity of methods[54,55].

Brownian dynamics simulations have shown shear thinning behaviour[33] but not shear thickening probably because the above algorithm has no inertia in the dynamics. It has been used to investigate the rheology of model stable suspensions[56], and flocculated suspensions (electro-rheological fluids and depletion flocs)[57,58]. At high shear rates (in the second Newtonian plateau) structures similar to those produced using the gaussian thermostat in *NEMD* have been observed. The distance and time scales of the model colloidal particles are minutes and μm, so comparison with experiment is feasible whereas it is not for the atomic fluids modelled by *NEMD*. A picture is now evolving of a strong link between microstructural changes under shear flow and the observed rheology. Neutron and light scattering, combined with brownian dynamics computer simulations, are proving effective complementary tools in bridging the microscopic and macroscopic behaviour of colloidal systems. One structural probe that can be accessed by both scattering experiments and *BD* is the Fourier transform of $g(\mathbf{r}, \dot{\gamma})$,[59]

$$S(\underline{k}) = S_0(k) + Pe\frac{k_x k_y}{k^2} A_1(k,\phi) + Pe^2 \frac{k_x^2}{k^2} A_1(k,\phi) + Pe^2 \frac{k_x^2 k_y^2}{k^4} A_2(k,\phi) + \cdots \quad (6.35)$$

where $A_1(k,\phi)$ and $A_2(k,\phi)$ are state dependent variables. A typical schematic picture of the scattering beam and couette cell is shown in Figure 4[60]. In practice it is difficult to probe the shear-gradient plane, the flow-vorticity direction being easier. Neutron scattering has given evidence that the 'density' of particles in the flow direction diminishes and in the vorticity direction it increases. This picture is entirely consistent with the string phase, as revealed by *BD* as the average density of particles along the string diminishes with increasing shear rate and the number of strings per unit volume increase[56].

Over the complete volume fraction range the following analytic expressions, called the Krieger-Dougherty equations, fit the experimental relative viscosity data of near hard-sphere dispersions quite well,[61]

$$\eta_{r0} = (1 - V_f/0.63)^{-2}, \quad (6.36)$$

and

$$\eta_{r\infty} = (1 - V_f/0.71)^{-2}, \quad (6.37)$$

where $\eta_{r\infty}$ is the relative viscosity of the colloidal liquid in the second Newtonian plateau. As there are no many-body hydrodynamics in the simulation, it gives the relative viscosity difference, $\eta_{r0} - \eta_{r\infty}$, rather than η_{r0} ($\eta_{r\infty}$ is entirely hydrodynamic in origin). A recent extension of *BD* to consider oscillatory shear has been made[62]. The analytic expressions for the dynamic moduli are, for the storage modulus, G',

$$G' = \frac{\omega}{n\pi\gamma_0} \int_0^{2n\pi/\omega} \sigma_{xy}(t')\, dt' \cos(\omega t'), \quad (6.38)$$

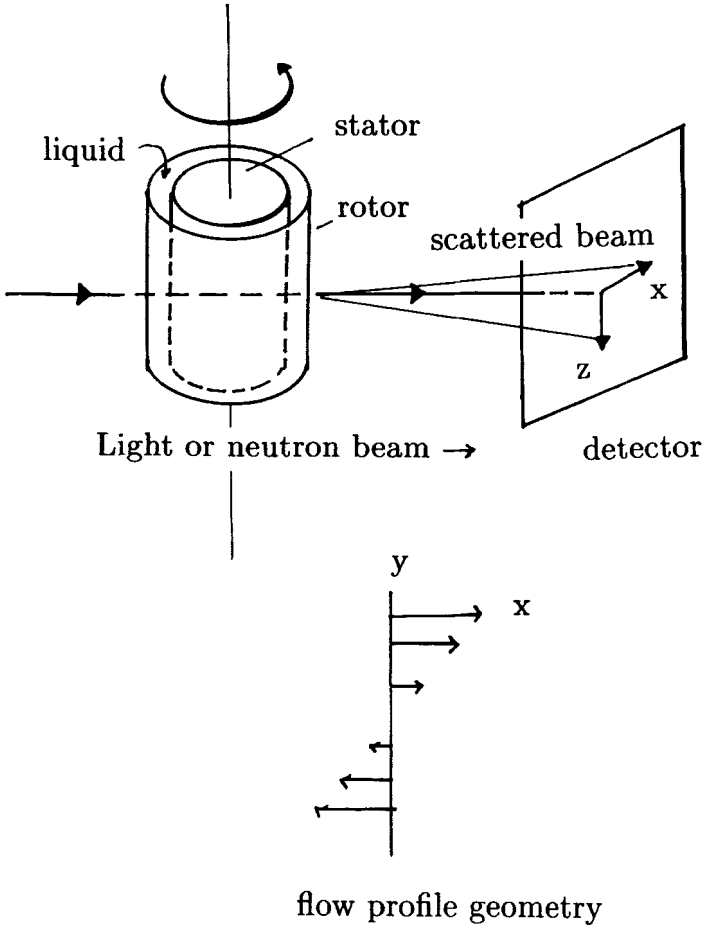

Figure 4 A sketch of the typical arrangement used for light or neutron scattering of colloidal liquids under shear.

and for the loss modulus G'',

$$G'' = \frac{\omega}{n\pi\gamma_0}\int_0^{2n\pi/\omega} \sigma_{xy}(t')dt' \sin(\omega t'). \tag{6.39}$$

The contents of the cell are homogeneously strained in an oscillatory fashion over n cycles and these integrals are evaluated numerically. The imaginary viscosity difference, $\eta' = G''/\omega$, for a $\phi = 0.427$ state using a $\phi(r) = k_B T(\sigma/r)^{36}$ potential is shown in Figure 5, taken from this programme of work. In the limit of zero frequency this should give the Newtonian viscosity. The prediction based on the Krieger-Dougherty formulae is given on the Figure. It can be seen that, even without many-body hydrodynamics in the model, the extrapolation as $\omega \to 0$ is in good agreement with the experimental value.

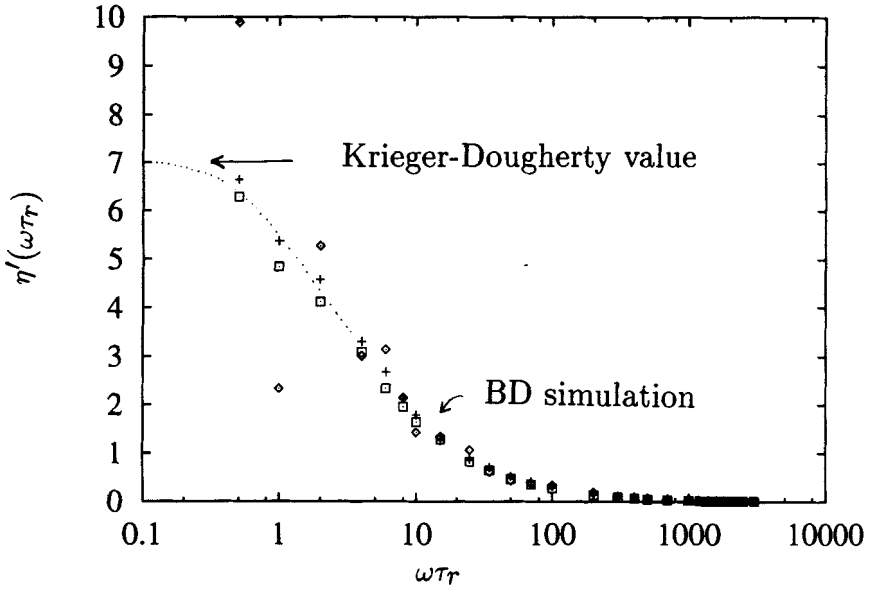

Figure 5 The frequency dependence of the imaginary viscosity, η' as a function of frequency for three strain amplitudes, (a) $\gamma_0 = 0.02$, (diamond) (b) $\gamma_0 = 0.10$ (cross) and (c) $\gamma_0 = 0.25$ (square) at $\phi = 0.472$, $N = 108$ and interaction cut-off at $r_c = 1.1\sigma$ for a r^{-36} pair potential.

To summarize, this section has described the progress made by molecular simulation in modelling non-Newtonian flow. The molecular simulation approaches are useful in providing a microscopic interpretation of the origins of non-Newtonian flow, and offer an exciting prospect for the future.

7 INTERFACIAL TRANSPORT AND RHEOLOGY

The physics of the interfacial region separating two fluids is an area of considerable current interest at the time of writing. The area embraces soft condensed matter, and in particular complex fluids such as liquid-liquid emulsions and gas-liquid forms. Interfacial rheology is concerned with the response of mobile interfaces to deformation.

To begin a discussion of interfacial transport, one is concerned with the theory, measurement and application of interfacial hydrodynamics. One can start by adopting the classical macroscopic view of fluid interfaces as idealized two-dimensional singular surfaces. The adsorption of molecular or macromolecular surfactants imparts intrinsic rheological properties to the interface such as interfacial shear and dilatational viscosities (which are two-dimensional counterparts of the three-dimensional viscosities treated above) and Gibbs elasticity, which indicates the change in interfacial tension with area. Gradients in surfactant concentration and temperature cause interfacial tension gradients that produce such phenomena as the 'tears' of strong wine.

As to experiment, light-scattering techniques have acquired considerable importance, (see, e.g. Dorshow and Turkevich[63]), as has the deep-channel viscometer for measuring interfacial shear viscosity. This is defined as the ratio of interfacial shear stress to rate of shear.

As part of the above general area, one can cite important applications including Rayleigh and Benard instabilities, interfacial turbulence, thin-liquid-film hydrodynamics and stability and the rheology and stability of foams and emulsions. The understanding of the metastability of complex fluids, involving the use of Derjaguin-Landau-Verwey-Overbek theory, is important to pure scientists and technologists alike. The reader wishing to go further should consult the edited volume by Edwards, Brenner and Wasan[14].

8 SUMMARY AND PROPOSALS FOR FUTURE WORK

While, for Newtonian liquids, a good deal of urderstanding now exists of mechanical properties, there remain diffuculties for a fully analytical theory, and most formulae that have emerged are still based on models (eg hard sphere models on the one hand, cage models, and models most appropriate for simple liquid metals with soft cores and long-range forces based on spectral functions with relatively sharp cut-off at a 'Debye' frequency.) Though computer simulation has helped greatly in classes of liquids such as Lennard-Jones fluids, and in clarifying between various transport formulae proposed (see, for example, Allen[64]), the need for analytical progress remains a focal point. On the experimental side, a systematic programme of experimental studies of bulk viscosity on simple liquids seems called for, though the experimental measurement still seems rather difficult.

Of course, the field of non-Newtonian liquids remains much more open theoretically, and much further work is called for here, both computational and analytical. Again, systematic experimental programmes seem called for, to test, and if necessary, allow extensions of current concepts and models. The area of non-Newtonian liquids is currently of great technological importantance, as is that of rheological behaviour at interfaces (see the book by Edwards *et al.*[14]).

References

1. S. Chapman and T. G. Cowling, The Mathematical Theory of Non-Uniform Gases (Cambridge: University Press), 1960.
2. J. H. Irving and J. G. Kirkwood, *J. Chem. Phys.* **18**, 817 (1950).
3. H. N. V. Temperley and D. H. Trevena, Liquids and Their Properties (Ellis Horwood: Chicester), 1978.
4. F. C. Collins and H. Raffel, *J. Chem. Phys.* **22**, 1728 (1954).
5. H. C. Longuet-Higgins and J. A. Pople, *J. Chem. Phys.* **25**, 884 (1956).
6. See, for instance, J. P. Hansen and I. R. McDonald, Theory of Simple Liquids (Academic: New York), 1976.
7. J. A. Ascough, R. G. Chapman and N. H. March, *Phys. Chem. Liquids*, **18**, 253 (1988).
8. R. Zwanzig, *J. Chem. Phys.* **79**, 4507 (1983).
9. R. C. Brown and N. H. March, *Phys. Chem. Liquids* **1**, 1411 (1968).
10. E. N. da C. Andrade, *Phil. Mag.* **17**, 497 (1934).
11 L. van Hove, *Phys. Rev.* **93**, 1374 (1954).

12. P. A. Egelstaff, An Introduction to the Liquid State: 2nd Edition (Oxford: Clarendon Press) 1992.
13. N. H. March, Liquid Metals: Concepts and Theory (Cambridge: University Press), 1990.
14. D. A. Edwards, H. Brenner and D. T. Wasan, Interfacial Transport Processes and Rheology (Butterworth-Heinemänn: Boston USA), 1991.
15. M. H. Ernst, E. H. Hauge, and J. M. J. Van Leeuwen, *Phys. Rev. Lett.* **25**, 1254 (1970).
16. T. Gaskell and N. H. March, *Physics Letters* **33A**, 460 (1970).
17. N. H. March, *J. Chem. Phys.* **80**, 5345 (1984).
18. A. Rahman, *Phys. Rev.* A **136**, 405 (1964).
19. D. Levesque, L. Verlet and J. Kurkijavi, *Phys. Rev.* **A7**, 1690 (1973).
20. D. Levesque and L. Verlet, *Molecular Physics* **61**, 143 (1987).
21. M. Ferrario, G. Ciccotti, B. L. Holian and J.-P. Ryckaert, *Phys. Rev.* **A44**, 6936 (1991).
22. P. Borgelt, C. Hoheisel and G. Stell, *Phys. Rev.* **A42**, 789 (1990).
23. K. D. Hammonds and D. M. Heyes, *JCS Faraday Trans. II* **84**, 705 (1988).
24. R. Vogelsang, G. Hoheisel and M. Luckas, *Molecular Physics* **71**, 781 (1990).
25. D. M. Heyes and J. G. Powles, *Molecular Physics* **71**, 781 (1990).
26. E. M. Gosling, I. R. McDonald and K. Singer, *Mol. Phys.* **26**, 1475 (1973).
27. W. T. Ashurst and W. G. Hoover, *Phys. Rev. A* **11**, 658 (1975).
28. A. W. Lees and S. F. Edwards, *J. Phys. C* **5**, 1921 (1972).
29. D. J. Evans and G. P. Morriss, *Phys. Rev. A* **30**, 1528 (1984).
30. W. G. Hoover, A. J. C. Ladd and B. Moran, *Phys. Rev. Lett.* **48**, 1818 (1982).
31. D. J. Evans and G. P. Morriss, *Phys. Rev. Lett.* **56**, 2172 (1986).
32. W. G. Hoover, *Phys. Rev. A* **40**, 2814 (1989).
33. D. M. Heyes, *J. Non-Newt. Fl. Mech.* **27**, 47 (1988).
34. D. J. Evans, H. J. M. Hanley and S. Hess, *Phys. Today* **37**, 26 (1984).
35. M. Ferrario, G. Ciccotti, B. L. Holian, and J.-P. Ryckaert *Phys. Rev. A* **44**, 6936 (1991).
36. D. J. Evans and G. P. Morriss, *Phys. Rev. A*, **38**, (1988) 4142; see also D. J. Evans and G. P. Morriss, 'Statistical Mechanics of Nonequilibrium Liquids', Academic Press, London, 1990.
37. S. Chynoweth, U. C. Klomp and Y. Michopoulos, *J. Chem. Phys.* **95**, 3024 (1991).
38. J. Z. Xue, E. Herbolzheimer, M. A. Tutgers, W. B. Russel and P. M. Chaikin, *Phys. Rev. Lett.*, **69**, 1715 (1992).
39. A van Blaaderen, J. Peetermans, G. Maret and J. K. G. Dhont, *J. Chem. Phys.*, **96**, 4591 (1992).
40. J. W. Goodwin and R. H. Ottewill, *J. Chem. Soc., Faraday Trans.*, **87**, 357 (1991).
41. R. H. Ottewill, *Langmuir*, **5**, 4 (1989).
42. G. T. Evans and C. P. James, *J. Chem. Phys.* **79**, 5553 (1983).
43. R. Simon, T. Palberg and D. Leiderer, *J. Chem. Phys.* **99**, 3030 (1993).
44. K. R. Harris, *Mol. Phys.* 77, 1153 (1992).
45. R. Buscall, *JCS, Faraday Trans*, **87**, 1365 (1991).
46. R. J. Speedy, *Mol. Phys.*, **62**, 509 (1987).
47. J. J. Erpenbeck and W. W. Wood, *Phys. Rev. A* **43**, 4254 (1991).
48. J. L. Hildebrande, *Science*, **174**, 490 (1971).
49. J. H. Dymond, *Physica B* **144**, 267 (1987).
50. K. D. Hammonds and D. M. Heyes *J. Chem. Soc. Faraday Trans 2* **84**, 705 (1988).
51. T. Akesson and B. Jonsson, *Mol. Phys.* **54**, 369 (1985).
52. W. Hess and R. Klein *Adv. in Phys.* **32**, 173 (1983).
53. D. L. Ermak, *J. Chem. Phys.* **62**, 4189 (1975).
54. G. Bossis and J. F. Brady, *J. Chem. Phys.* **91**, 1866 (1989).
55. P. J. Hoogerbrugge and J. M. V. A. Koelman, *Europh. Lett.* **19**, 155 (1992).
56. D. M. Heyes, and J. R. Melrose, *J. Non-newt Fl. Mech.* **46**, 1 (1993).
57. J. R. Melrose and D. M. Heyes, *J. Chem. Phys.*, **98**, 5873 (1993).
58. J. R. Melrose and D. M. Heyes *J. Coll. & Interface Sci.* **157**, 227 (1993).
59. C. G. de Kruif, J. C. van der Werff, S. J. Johnson and R. P. May, *Phys. Fluids. A* **2**, 1545 (1990).
60. R. H. Ottewill and A. R. Rennie, *Int. J. Multiphase Flow*, **16**, 681 (1990).
61. W. B. Russel, D. A. Saville, and W. R. Schowalter, "Colloidal Dispersions", Cambridge Univ. Press, 1989, p. 466.
62. P. B. Visscher, P. J. Mitchell and D. M. Heyes, *Progr. Coll. & Pol. Sci.*, submitted.
63. R. Dorshow and L. Turkevich, *J. Chem. Phys.* **98**, 5762 (1993).
64. M. P. Allen, Molecular Physics, 1993, to appear.